Cooperative Adaptive Cruise Control for Connected Autonomous Vehicles using Spring Damping Energy Model

Songtao Xie, Junyan Hu, *Member, IEEE*, Zhengtao Ding, *Senior Member, IEEE*, and Farshad Arvin, *Senior Member, IEEE*

***Abstract*—Cooperative adaptive cruise control (CACC) has been widely considered as a potential solution for reducing traffic congestion, increasing road capacity, reducing fossil fuel consumption and improving traffic safety. Traditional CCAC methods rely heavily on the vehicle-to-vehicle communications to achieve cooperation. However, in the real-world scenarios, unreliable communication will degrade CACC to adaptive cruise control, which may bring negative influences on safety (i.e., increase the risk of collisions). To overcome this drawback, this paper innovatively applies a spring damping energy model to construct a robust autonomous vehicle platoon system. The proposed design of the energy model ensures that the stability and safety of the platoon system be maintained in the event of such sudden degradation. Based on this technique, a distributed control protocol which only utilizes local information from neighbors is then proposed. Furthermore, some practical constraints such as the connectivity of the vehicle platoon system and the bound of the control inputs are guaranteed. Finally, the effectiveness of the proposed CCAC strategy is validated by multiple simulation experiments in Unreal Engine.**

***Index Terms*—Autonomous vehicles, cooperative adaptive cruise control, distributed multi-vehicle systems, spring damping energy model, vehicle-to-vehicle communication.**

I. Introduction

Cooperative Adaptive Cruise Control (CACC) enables longitudinal automation of connected vehicle platoons by utilizing inter-vehicle distances and vehicle state information, which can be obtained by equipped radars and vehicle-to-vehicle (V2V) communication modules [1], [2]. This technique is able to maintain a suitable inter-vehicle distance to alleviate traffic congestion, improve safety, fuel economy and traffic throughput [3]–[6].

In recent years, a large number of scholars have conducted research on CACC with remarkable success. The traditional proportional-integral-derivative control design has been widely used as an effective method in Adaptive Cruise Control (ACC) and CACC, which is also the control scheme now used by most mainstream automobile original equipment manufacturers [2]. In the implementation of the proportional-integral-derivative control, the control input (such as acceleration or velocity) of an individual vehicle is obtained by a nonlinear function, using either the constant spacing strategy or the constant time headway strategy [7], [8]. Model predictive control (MPC) is also widely adopted in CACC schemes. These control methods not only take V2V spacing as a control objective, but also consider more optimization indicators such as energy consumption [9], [10], comfort [11], and traffic efficiency [12]. Nowadays, a more mainstream approach is to combine distributed mechanism with MPC [13]–[15]. Other control methods are also being investigated, in [16], the stochastic optimal control strategy can produce smoother vehicle control input signal with small system disturbances and large measurement disturbances. In [17], a new control structure with optimal control and online learning is used to find the optimal error feedback, as well as seek the minimum headway values. In addition, control methods based on a combination of data-driven and optimization are gaining more and more attention from researchers, where reinforcement learning-based techniques have been utilized in many studies [18]–[20] as a potential solution to achieve CACC. However, these optimization-based control algorithms and data-driven approaches place enormous demands on the computing capacity of the autonomous vehicles.

CACC is a framework that relies heavily on the V2V communication. If the V2V communication is attacked or lost, CACC will degrade to ACC, thus increasing the risk of vehicle collisions [21]–[24]. Numerous experimental results have shown that ACC has a negative impact on the traction energy consumption of the vehicle [25], [26]. In addition, more real vehicle experiments and empirical data are needed to support the improvement and optimization of the ACC model [27]. To overcome this issue, some preliminary results have been obtained by researchers in recent years. In [28], by incorporating statistical learning with the physical laws of kinematics, a real-time anomaly detection mechanism is proposed which has shown to be effective in detecting forgery attacks in CACC. Besides, the association between multiple motion parameters concerning both individual and consecutive vehicle is used to assess the credibility of the information provided by the connected members [29]. The security of V2V communications has been assured with the emphasis placed on cyber security by original equipment manufacturers [30], such as by introducing of secure onboard

The second and last authors were supported by EU H2020-FET-OPEN RoboRoyale project [grant number 964492].

S. Xie and Z. Ding are with the Department of Electrical and Electronic Engineering, The University of Manchester, Manchester, M13 9PL, UK. (e-mail: {songtao.xie, zhengtao.ding}@manchester.ac.uk)

J. Hu is with the Department of Computer Science, University College London, London, WC1E 6BT, UK. (e-mail: junyan.hu@ucl.ac.uk)

F. Arvin is with the Swarm & Computational Intelligence Laboratory (SwaCIL), Department of Computer Science, Durham University, Durham, DH1 3LE, UK. (e-mail: farshad.arvin@durham.ac.uk)

communication [31]. These encrypted communications protect the authenticity of communication messages to a large extent. Hence, communication loss has now become the leading cyber security issue in CACC. In order to completely avoid the communication loss problem, it is necessary to expand the communication infrastructure and reduce the failure rate of the onboard communication modules [32]. However, for the CACC algorithm, improving the algorithm to reduce or eliminate the negative effect of communication loss may be more feasible and efficient [33], [34]. In [35], the researchers model communication losses as independent random events. By applying H_∞ control tools to the both plant stability and string stability of the average error dynamics and minimizing the variance of the trajectories, the effect of the communication losses can be effectively mitigated. A disturbance observer-based sliding mode control is proposed in [36], which estimates the uncertainty present in the actuator dynamics and the acceleration of the preceding vehicle as a lumped disturbance. In addition, state estimation is considered to be an effective solution to temporary loss of communication [37]. When the V2V communication is temporarily lost, [38] utilizes an adaptive Kalman filter to estimate the acceleration of a preceding vehicle, and the estimated acceleration is implemented as a feedforward signal in the ego-vehicle CACC design. However, most of these solutions are simply finding an estimate for the vehicle to use as a feedback input to achieve CACC. When the number of vehicles experiencing a loss of communication increases, it will bring more difficulties for these methods to secure the system.

Motivated by the aforementioned challenges, we aim to propose a reliable CCAC framework by using Spring Damping Energy Model (SDEM) and distributed mechanisms. Different from traditional methods, in our solution, we do not perform state estimation in the case of communication loss. Instead, we aim to design a more generalized CACC algorithm, i.e. one applicable to CACC and equally applicable to ACC. In addition to achieving basic obstacle avoidance and vehicle speed consistency, the proposed control design can also achieve the boundedness of the control input and maintain the connectivity of the topology. To the best of authors' knowledge, such a SDEM-based distributed control strategy has not been developed in the literature. This paper draws on the network model presented in [37], [39]. On-board sensors can acquire information about the movement of the closet front vehicle, while V2V communication can obtain state information about the movements of all vehicles within the communication range. The main contributions of the paper are as follows:

- We innovatively use a specially defined SDEM to construct a robust self-driving vehicle platoon system. This model ensures the internal stability of the platoon system, the stability of the topology connections, and the consistency of the platoon velocity.
- A special nonlinear spring is designed to describe the V2V interaction, which can ensure that no collision occur within the platoon. Besides, the desired speed can be maintained in the presence of sudden acceleration or deceleration by the leading vehicle.
- Based on the proposed energy model, a distributed control protocol is proposed, which only relies on state information from neighboring vehicles. The string stability of the vehicle system under this control protocol is proved. Also, this generalized control protocol can be applied to both CACC and ACC cases.
- The effectiveness of the proposed strategy under several scenarios (including merging and separating) is verified by realistic simulation experiments, which lays the foundation for implementing it on a real vehicle platoon in the future.

The rest of this paper is structured as follows: Preliminaries and problem statements are shown in Section II. We propose the distributed control protocol based on the SDEM and prove the stability of the control protocol in Section III. The experimental results are analyzed and discussed in SectionIV. Finally, we conclude this work in SectionV.

II. Problem formulation

A. Dynamics Model

In the current studies on CACC, the linearization technique is commonly applied to deal with the upper-level longitudinal nonlinear dynamics [40], [41]. Since we mainly focus on developing high-level multi-vehicle coordination strategies in this paper, to simplify the dynamics model, the air drag, rolling resistance, and actuator delay in the vehicle dynamics model are ignored. The second-order differential model can be described using ordinary differential equations (ODE) following [42]:

$$\begin{cases} \dot{x}_i = v_i \\ \dot{v}_i = u_i \end{cases}, \tag{1}$$

where x_i, v_i and u_i are the position, velocity and control input of vehicle i, respectively.

B. Communication Topology and Vehicle Platoon

A time-varying directed graph $\mathcal{G}(t) \triangleq (\mathcal{V}, \mathcal{E}(t))$ is used to describe the network topology among the vehicles within the platoon, where $\mathcal{V} \triangleq \{\mathcal{V}_1, \ldots, \mathcal{V}_N\}$ is set of nodes. And the element of $\mathcal{E}(t) \in N \times N$ is denoted as $(\mathcal{V}_i, \mathcal{V}_j)$, which is termed an edge from $\mathcal{V}_i$ to $\mathcal{V}_j$. $A(t) = [a_{ij}] \in \mathbb{R}^{N\times N}$ is the adjacency matrix of graph $\mathcal{G}(t)$. $a_{ij} = 1$, if $\|x_i(t) - x_j(t)\| < \rho$, otherwise, $a_{ij} = 0$. $a_{ij} = 1$ means that the vehicles i can receive the information from vehicle j through V2V communication or on-board sensors. In this paper, we suppose that the initial connection topology of vehicle platoon is connected. The initial connection of the system is: $\mathcal{E}(0) = \{(i,j), | \, \|x_i(0) - x_j(0)\| < \rho, i, j \in \mathcal{V}\}$.

We consider a platoon of $N+1$ vehicles with index from 0 to N as shown in Fig. 1. The index 0 represents the leader and index 1 to N denote the followers. l_i is the body length of vehicle i. x_i and v_i, respectively, are the position and velocity of the front bumper of vehicle i. $S_i := x_i - x_{i-1} - l_{i-1}$ is the distance between the front bumper of vehicle i and the back bumper of the vehicle $i-1$. The vehicle can obtain the motion state of the nearest vehicle in front by the ob-board

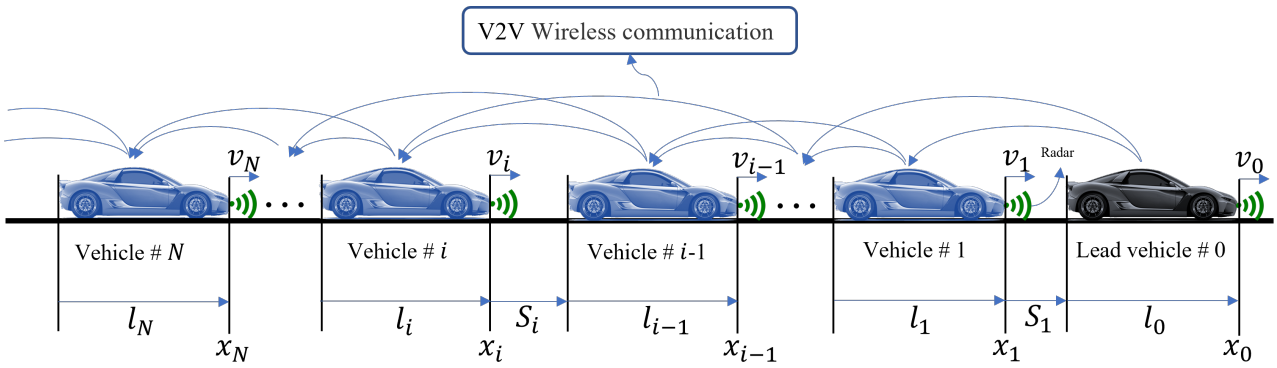

Fig. 1. Network topology model for autonomous vehicle platoon

sensors (e.g., radar) and the V2V communication, including position and speed information, and obtain the motion state of the vehicles beyond the radar field of vision through V2V communication. Define a variable to denote the desired distance between vehicle i and vehicle j:

$$\hat{S}_{ij} = \sum_{k=j+1}^{i} S_k + \sum_{k=j}^{i-1} l_k \quad \forall i > j \geq 0\,, \tag{2}$$

where S_k represents the desired distance between the vehicle k and vehicle $k-1$. In addition, suppose that the V2V communication radius is ρ, therefore, the number of vehicles which are within the communication range of vehicle i is limited. Assume that this limited number is m. In the proposed algorithm in this paper, we assume that the connection topology between vehicle platoon is directional. This means that vehicle i can use the state information from vehicle j, while vehicle j does not use the state information from vehicle i, $\forall i > j \geq 0$.

C. Control Objectives

For a vehicle platoon with a leader having constant velocity v_o, when the initial connection topology is connected, the objective is listed as follows:

- To achieve the following steady state:

$$\begin{cases} \lim_{t\to\infty} \|x_i(t) - x_j(t)\| = \sum_{k=j+1}^{i} S_k + \sum_{k=j}^{i-1} l_k \\ \lim_{t\to\infty} \|v_i(t) - v_0(t)\| = 0 \end{cases} \quad \forall i > j \geq 0. \tag{3}$$

  This control objective implies that the following distance and speed of all vehicles within the platoon need to converge to the desired value.
- From the perspective of functional security, the temporarily loss of V2V communication may lead to platoon collision. Therefore, another important control objective is that when V2V communication is lost, the connection topology of the platoon does not completely disconnect and the vehicle platoon continues to converge to the desired steady state.
- Topology connectivity within the platoon can be guaranteed despite sudden acceleration or deceleration by the leading vehicle. And the vehicle platoon system can re-enter the steady state within a finite time.

D. Basic Lemmas

To facilitate further proof, we introduce the following lemma.

Lemma 1 ([43]): L has rank $N-1$, i.e., $\lambda_1 = 0$, if and only if graph $\mathcal{G}$ has a spanning tree. Where L is the Laplace matrix of $\mathcal{G}$, and λ_1 is the first eigenvalue of L.

Lemma 2 ([44]): For symmetric matrices $A, B \in \mathbb{R}^{N\times N}$, if their eigenvalue sequences satisfy $\lambda_1(A) \leq \cdots \leq \lambda_N(A), \lambda_1(B) \leq \cdots \leq \lambda_N(B)$, the following conclusions can be drawn:

$$\lambda_{i+j-1}(A+B) \geq \lambda_i(A) + \lambda_j(B), \tag{4}$$

where $i + j \leq N + 1, 1 \leq i, j \leq N$.

Lemma 3 ([44]): If the graph $\mathcal{G}$ is connected, there exists left eigenvector $y > 0$ of $L(\mathcal{G})$ such that $L^T(\mathcal{G})y = 0$, $y^T 1_N = 1$.

Additionally, we define the following lemma:

Lemma 4: For a connected graph $\mathcal{G}$, define:

$$\begin{aligned} P &= \operatorname{diag}\{p_i\} \in \mathbb{R}^{N\times N} \\ Q &= PL(\mathcal{G}) + L^T(\mathcal{G})P, \end{aligned} \tag{5}$$

where $p = [p_1, p_2, \ldots, p_N]$ is the left eigenvector corresponding to the zero eigenvalue of $L(\mathcal{G})$, such that $Q \geq 0$, Q has rank $N-1$.

Proof: According to the definition of Laplace matrix, we can get:

$$\begin{aligned} L(\mathcal{G}) &= \operatorname{diag}\{d_i\} - A \\ L^T(\mathcal{G}) &= \operatorname{diag}\{d_i\} - A^T, \end{aligned}$$

where A and $\operatorname{diag}\{d_i\}$ are, respectively, the adjacency matrix and in-degree matrix of graph $\mathcal{G}$. Hence,

$$PL(\mathcal{G}) + L^T(\mathcal{G})P = \operatorname{diag}\{2d_i p_i\} - (PA + A^T P).$$

The sum of i^{th} row is $2d_i p_i + \sum_{j=1}^{N}(a_{ij}p_i + a_{ji}p_j)$. Because $L^T(\mathcal{G})p = 0$, $d_i + \sum_{j=1}^{N} a_{ji}p_j = 0$, we can obtain that the sum of i^{th} row is 0:

$$Q \begin{pmatrix} 1 \\ \vdots \\ 1 \end{pmatrix}_N = \begin{pmatrix} 0 \\ \vdots \\ 0 \end{pmatrix}_N .$$

Due to $Q^T = Q$, we also get:

$$(1, \ldots, 1)_N Q = (0, \ldots, 0)_N.$$

Hence, Q is the Laplace matrix of graph $\bar{\mathcal{G}}$, the weighted mirror graph of a connected directed graph $\mathcal{G}$. The weight of edge (i, j) is $\bar{a}_{ij} = p_i a_{ij} + a_{ji} p_j$. We can conclude that $\bar{\mathcal{G}}$ is a strongly connected un-directed graph. The rank of Q is $N - 1$, and $Q \geq 0$. Thus, the proof is done. ■

III. Cooperative Adaptive Cruise Control Design

In this section, we design a distributed cooperative control protocol for the vehicle platoon system from the perspective of system energy. This novel control design is capable of achieving all our pre-specific control objectives.

A. Spring Damping Energy Model

In this paper, we consider a platoon system from a very novel perspective, i.e., system energy. We start by constructing a single spring damping energy system, such as the subsystem in Fig. 2, consisting of A_1, A_2, K_{12}, and c_{12}. Define A, c, and K as, respectively, the agents, damping elements, and spring elements. In addition, we define energy in the energy model as follows:

$$\begin{aligned} E_A(t) &= \frac{1}{2} v(t)^2 \\ E_K(t) &= g(\Delta l_A(t)) \\ E(t) &= E_A(t) + E_K(t), \end{aligned} \tag{6}$$

where $E_A(t)$, $E_K(t)$, and $E(t)$ are, respectively, the kinetic energy of agents, potential energy stored in the spring, and total current energy of the system. $\Delta l_A(t)$ denotes the distance between agents, and g is a function of $\Delta l_A(t)$.

Lemma 5: For the energy system defined above, assume that the system has finite initial energy, the system will achieve asymptotic stability in the absence of external energy input.

Proof: The time-varying energy function of the system is as follows:

$$E(t) = \frac{1}{2} v_1(t)^2 + \frac{1}{2} v_2(t)^2 + g(\Delta l_A). \tag{7}$$

In this spring damping system, the damping unit and the spring unit together provide acceleration to the agents, which satisfies the following equation

$$a = -\nabla g - c \Delta v, \tag{8}$$

where $c > 0$ is the damping coefficient. The derivative of this function with respect to time gives:

$$\begin{aligned} \dot{E}(t) &= v_1(-\nabla g - c\Delta v) + v_2(+\nabla g + c\Delta v) + \Delta v \nabla g \\ &= -c\Delta^2 v \leq 0, \end{aligned} \tag{9}$$

which means the system energy is progressively stable. The derivative of (7) with respect to time shows that the spring damping energy system will converge to a steady state where $\Delta v(t)$ equals 0, and $\Delta l_A(t)$ equals constant. ■

Based on the above definition, we take such a basic spring-damping energy system unit and form it into a more complex energy system by connecting it in series and parallel. We consider using a particular spring-damping energy model (shown as Fig. 3) to simulate a vehicle platoon system with no external energy input. A_1, A_2, A_3 represent the agents corresponding to the vehicle in the vehicle platoon system. In this model, K is a specially designed nonlinear spring that also acts as an energy storage element. c represents a damper, which is an energy-consuming element whose rate of energy consumption depends on the velocity difference between agents. The storage element K is assigned specific storage limits $E_{max} + e_1$, where E_{max} denotes the initial energy of the entire system, including the kinetic energy of agents and the potential energy already stored in K, and e_1 is a constant to ensure that the actual energy storage of the spring does not exceed the maximum value. According to (9), the multi-vehicle system constitutes an energy consuming system. In the absence of external energy input, the system energy always decreases or maintains a steady state during the task. Therefore, when the total energy of the system is transferred to one spring unit, the energy stored in the spring will not exceed the spring's storage limit. The energy stored in K is a specific function of the distance between the agents. When there is a velocity difference between agents, the energy consuming element c will keep consuming energy. According to the most fundamental law of thermodynamics, in the absence of external energy input, the system's total energy will not increase and may decrease due to the presence of energy-consuming elements. The rest of the energy in the system consists of the energy stored in the spring and the kinetic energy of the agent, which are dynamically converted to each other.

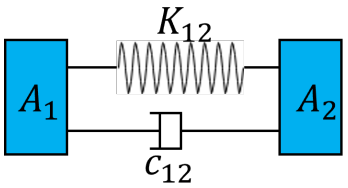

Fig. 2. A single spring damping energy system.

According to the conditions mentioned above, since the system's total energy is always less than or equal to the initial energy of the system, the actual energy stored by the spring can never reach its limit. This property means that the stretch and compression of the spring will not exceed the limited length. In addition, the steady state of the system is achieved when the energy storage of the spring is zero, and the energy consumption of the energy-consuming element is also zero. The above conclusion corresponds to the vehicle platoon system, the distance between vehicles will not be less than the minimum allowable distance, nor will the communication connection be disconnected. The vehicle platoon converges to a state where the velocities of the vehicles are consistent, and the distance between the vehicles satisfies expectations.

B. Distributed Control Protocol

This section aims to develop distributed cooperative control algorithm for connected vehicle platoons to achieve the

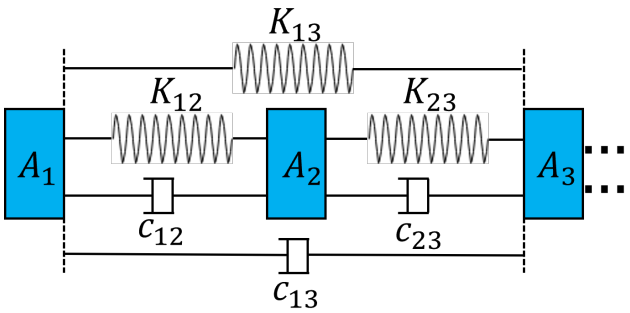

Fig. 3. A complex spring damping energy model to describe a vehicle platoon system

following control objectives:

- Given a leading vehicle with a constant velocity, the velocities of all followers should converge to the leader's velocity.
- In the vehicle platoon, the following distance between all vehicles should be stable and converge to the expected value.
- When V2V communication is lost, the vehicle platoon should still achieve the desired queue.
- The string stability of the platoon must be ensured when there is a sudden change in velocity of the leader.
- The connectivity of topology should be guaranteed.

The control protocol we designed is given as follows

$$\begin{aligned} u_i = &- \sum_{j\in\mathcal{N}_i} \nabla x_i V_{ij} \left| \sum_{j\in\mathcal{N}_i} a_{ij}(v_i - v_j) \right| - \beta \sum_{j\in\mathcal{N}_i} a_{ij}(v_i - v_j) \\ &- \frac{1}{2}\Big(\sum_{j\in\mathcal{N}_i\cup\{l\}} \nabla_{x_i} V_{ij}\Big) - h_i(v_i - v_0), \end{aligned} \tag{10}$$

where $h_i(t) = \begin{cases} 1 & i \in \mathcal{N}_l(t) \\ 0 & \text{others} \end{cases}$, β is the control gain, $\mathcal{N}_l$ denotes the set of neighbors of the leading vehicle. $\mathcal{N}_i$ represents the set of neighbors of the vehicle i, and the communication connection between vehicle i and vehicle j is directional. $\beta(v_i - v_j)$, and $v_i - v_0$ correspond to the damping energy dissipation function in the energy model. $-\sum_{j\in\mathcal{N}_i} \nabla x_i V_{ij} \left|\sum_{j\in\mathcal{N}_i} a_{ij}(v_i - v_j)\right|$ is the product of gradient and velocity difference, which can accelerate the convergence of the vehicle platoon system. V_{ij} is the interaction potential function between vehicles, corresponding to the spring energy function in the energy model. The gradient of V_{ij} is used to achieve obstacle avoidance and distance convergence of the vehicle platoon system. In this case, the interaction field function has to generate repulsive force over the interval $\left[l_j, \hat{S}_{ij}\right)$ and attractive force over the interval $\left[\hat{S}_{ij}, \rho\right)$. Hence, the specific form of the interaction potential function in this control protocol is designed as follows:

$$\begin{aligned} V_{ij}(\|x_{ij}\|) = &\frac{(\|x_{ij} - l_j\| - \hat{S}_{ij} + l_j)^2(\rho - \|x_{ij}\|)}{\|x_{ij} - l_j\| + \frac{(\hat{S}_{ij} - l_j)^2(\rho - \|x_{ij}\|)}{c_1 + \Psi_{max}}} \\ &+ \frac{\|x_{ij} - l_j\|\,(\|x_{ij}\| - \hat{S}_{ij})^2}{(\rho - \|x_{ij}\|) + \frac{\|x_{ij} - l_j\|(\rho - \hat{S}_{ij})^2}{c_2 + \Psi_{max}}}, \end{aligned} \tag{11}$$

where $\hat{S}_{ij}$ is given by (2), l_j is the length of vehicle j. Different from the commonly used interactive functions, in addition to meet the obstacle avoidance function. The potential field function can also achieve the boundedness of the control input and maintain the connectivity of the topology. Equation (11) is a smooth and bounded concave function. This function minimizes at $\|x_{ij}\| = \hat{S}_{ij}$, and is monotonically decreasing over the interval $\left[l_j, \hat{S}_{ij}\right)$ and monotonically increasing over the interval $\left[\hat{S}_{ij}, \rho\right)$. Ψ_{max} is the maximum of the system energy function, which is defined as follows

$$\begin{aligned} \Psi_{max} = &\frac{2mN - m^2 + m}{2} V_{max} \\ &+ \frac{1}{2}\sum_{i=1}^{N} \left(v_i(0) - v_0(0)\right)^2, 1 \le m \le N \end{aligned} \tag{12}$$

where $V_{max} = \max\{V(l_j + \xi_1), V(\rho - \xi_2)\}$. ξ_1 and ξ_2 are delay constants, used to ensure the stability of the topology connection. V_{max} is the value of the function V_{ij} at $x_{ij} = l_j + \xi_1$ or $x_{ij} = \rho - \xi_2$. It can be seen that V_{max} is not the endpoint value of the function V_{ij}. That is to say, V_{max} is always less than the endpoint value of the function V_{ij}. m is the maximum number of vehicles that can communicate with vehicle i.

According to the definition of SDEM, the maximum energy of the initial platoon system needs to be estimated. Here, we define system energy as consisting of the potential energy of the interaction field between vehicles and the squared deviation of the velocity. Then when the system is in the lowest energy state, the potential energy is zero, and the square of the velocity deviation is also zero. Hence, Ψ_{max} consists of all the interaction potential energy and velocity deviation energy in the system.

To facilitate the proof of the following theorems, we define:

$$f = \sum_{k=1}^{m} max(\|\nabla x_i V_{ik}\|). \tag{13}$$

As can be seen from the definition, f means the maximum interaction force of vehicle due to the potential field. In addition, we define a diagonal matrix as follows:

$$H = \text{diag}\left\{h_1(t_0), h_2(t_0), \ldots, h_N(t_0)\right\}. \tag{14}$$

Theorem 1: Suppose that the initial connection topology of the vehicle platoon $\mathcal{G}(t_0)$ is connected and the initial system energy $\Psi(t_0)$ is bounded. The connectivity of the time-varying network topology can be guaranteed if the following condition

$$\lambda_2((\beta Q + 2PH)(t_0)) > 4mf \tag{15}$$

is satisfied, where Q and P are defined in Lemma 4.

Proof: Let the follower's position and speed deviation from the leading vehicle be $\tilde{x}_i = x_i - x_0$ and $\tilde{v}_i = v_i - v_0$. Therefore, we have

$$\begin{aligned}
\dot{\tilde{x}}_i &= \tilde{v}_i \\
\dot{\tilde{v}}_i &= -\sum_{j\in\mathcal{N}_i} \nabla\tilde{x}_i\tilde{V}_{ij}\left|\sum_{j\in\mathcal{N}_l} a_{ij}(\tilde{v}_i-\tilde{v}_j)\right| \\
&\quad -\beta\sum_{j\in\mathcal{N}_l} a_{ij}(\tilde{v}_i-\tilde{v}_j) \\
&\quad -\frac{1}{2}(\sum_{j\in\mathcal{N}_l\cup\{l\}} \nabla_{\tilde{x}_i}\tilde{V}_{ij}) - h_i\tilde{v}_i.
\end{aligned} \tag{16}$$

Define the following non-negative energy function:

$$\Psi = \sum_{i=1}^{N} p_i \sum_{j\in\mathcal{N}_i\cup l} \tilde{V}_{ij}(\|\tilde{x}_{ij}\|) + \tilde{v}^{\mathrm{T}} P\tilde{v}, \tag{17}$$

where $\tilde{v} = [\tilde{v}_1, \ldots, \tilde{v}_N]^{\mathrm{T}}$.

Suppose $\mathcal{G}(t)$ will change its connection topology at t_e, $e = 1, 2, \ldots$, and the system connection topology $\mathcal{G}(t_e)$ will not change during $[t_e, t_{e+1})$. It's easy to verify that $\tilde{V}_{ij}$ is finite according to (11). Hence, $\Psi(t_0)$ (the initial value of the system energy function) is bounded. Take the derivative of the function in the interval $[t_0, t_1)$:

$$\begin{aligned}
\dot{\Psi} = &\sum_{i=1}^{N} \tilde{v}_i^{\mathrm{T}} p_i \sum_{j\in\mathcal{N}_l\cup\{l\}} \nabla\tilde{x}_i\tilde{V}_{ij} \\
&+ 2\tilde{v}^{\mathrm{T}} P \begin{pmatrix} -\beta L\tilde{v} - \mathrm{diag}\left\{\nabla\tilde{x}_i\tilde{V}_i\right\}|L\tilde{v}| \\ -\frac{1}{2}\nabla\tilde{V} - H\tilde{v} \end{pmatrix},
\end{aligned} \tag{18}$$

where

$$\begin{cases} \tilde{V}_i = \sum_{j\in\mathcal{N}_i} \tilde{V}_{ij} \\ \nabla\tilde{V} = \sum_{j\in\mathcal{N}_l\cup\{l\}} \nabla_{\tilde{x}_i}\tilde{V}_{ij}. \end{cases}$$

(18) can then be simplified as

$$\dot{\Psi} = 2\tilde{v}^{\mathrm{T}} P\left(-\beta L\tilde{v} - \mathrm{diag}\left\{\nabla\tilde{x}_i\tilde{V}_i\right\}|L\tilde{v}| - H\tilde{v}\right). \tag{19}$$

According to the definition of f in (13), we can obtain the following inequality

$$\left|\nabla\tilde{x}_i\tilde{V}_i\right| = \left|\nabla\tilde{x}_i\sum_{j\in\mathcal{N}_i}\tilde{V}_{ij}\right| \le f. \tag{20}$$

Hence, substituting (20) to (19), we have

$$\begin{aligned}
\dot{\Psi} &\le -2\tilde{v}^{\mathrm{T}} P\left(\beta L + H\right)\tilde{v} + 2f\|\tilde{v}\|\|P\|\|L\tilde{v}\| \\
&\le -\tilde{v}^{\mathrm{T}}\left(\beta Q + 2PH\right)(t_0)\tilde{v} + 2f\|\tilde{v}\|\|P\|\|L\|\|\tilde{v}\|.
\end{aligned} \tag{21}$$

According to the definition of Laplace matrix, we can get

$$L(\mathcal{G}) = \mathrm{diag}\{d_i\} - A,$$

where A and $\mathrm{diag}\{d_i\}$ are, respectively, the adjacency matrix and in-degree matrix of graph $\mathcal{G}$. According to the communication rules defined in Section II.B, we can determine that the adjacency matrix of the topology of vehicle platoon connection is a strict lower triangular matrix,

$$A = \begin{bmatrix} 0 & \cdots & \cdots & 0 \\ 1 & \ddots & & \vdots \\ \vdots & 1 & \ddots & \vdots \\ * & \cdots & 1 & 0 \end{bmatrix}, \tag{22}$$

where $*$ indicates that the value is uncertain and determined by the connection topology at a specific time, which is either 0 or 1. The matrix A indicates that the communication topology of the platoon is directional . Since $\mathrm{Max}\{d_i\} = m$, we have $\|L\| \le 2m$. Then (21) can be further rewritten as:

$$\begin{aligned}
\dot{\Psi} &\le -\tilde{v}^{\mathrm{T}}\left(\beta Q + 2PH\right)(t_0)\tilde{v} + 4mf\|\tilde{v}\|^2 \\
&\le -\left(\lambda_2\left(\beta Q + 2PH\right)(t_0) - 4mf\right)\|\tilde{v}\|^2.
\end{aligned} \tag{23}$$

Substituting the initial condition $\lambda_2((\beta Q + 2PH)(t_0)) > 4mf$, it gives

$$\dot{\Psi}(t) \le 0, \forall t \in [t_0, t_1), \tag{24}$$

which means that the $\Psi(t)$ is monotonically decreasing function in $[t_0, t_1)$. Take the derivative of (11), and we get that V_{ij} is monotonically decreasing over the interval $\left[l_j, \hat{S}_{ij}\right)$ and monotonically increasing over the interval $\left[\hat{S}_{ij}, \rho\right)$. Hence, following relationship can be obtained,

$$\begin{aligned}
&V_{ij}(\rho) \ge \Psi_{max} > \Psi(t_0), \forall (i,j) \in \mathcal{V} \\
&V_{ij}(l_j) \ge \Psi_{max} > \Psi(t_0), \forall (i,j) \in \mathcal{V}.
\end{aligned} \tag{25}$$

This indicates that the distance between the front bumper of vehicle i and vehicle j will not be l_j, which means the vehicle i will not contact the back bumper of vehicle j. On the other hand, the distance between vehicle i and vehicle j will not be equal to or bigger than the communication range ρ. This conclusion ensures that the topological connection of the vehicle platoon will not be interrupted in the process of system transformation over the interval $[t_0, t_1)$. Therefore, the platoon system can only establish new communication connections at time t_1. As a result, the connectivity of the system will be guaranteed. The proof of Theorem 1 is done. ■

String stability is an important indicator of the vehicle platoon system. In this paper, we use asymptotically time-domain string stability (ATSS) to analyze the string stability of the platoon system. According to the definition of ATSS in [45], the origin $e_i = 0$, $i \in \mathbb{N}$ of an interconnected system is ATSS if a given $\delta > 0$ is bounded. Hence we have

$$\sup_i |e_i(0)| < \delta \Longrightarrow \sup_i \|e_i(t)\|_\infty \to 0, \tag{26}$$

where $e_i = \tilde{x}_{ij} - \hat{S}_{ij}$. Based on the results obtained from Theorem 1, we can then have the following theorem.

Theorem 2: Consider a vehicle platoon system with time-varying topology defined in Theorem 1. Suppose that the initial connection topology of the vehicle platoon $\mathcal{G}(t_0)$ is connected and the initial system energy $\Psi(t_0)$ is bounded. If the condition (15) is satisfied, all vehicles' speeds will converge to the lead vehicle's speed. And the following distance between vehicles

will converge to the desired value. Meanwhile, the platoon system is ATSS.

Proof: We expand on the above proof using mathematical induction. Suppose that there are N_1 new connections being added to the platoon system at t_1. N_1 is limited, $\Psi(t_1) < \Psi(t_0) + N_1 V_{max}$, thus $\Psi(t_1)$ is also bounded. Lemma 4 indicates that $Q(t_1)$ is the Laplace matrix of graph $\mathcal{G}(t_1)$, the weighted mirror graph of a strongly connected directed graph $\mathcal{G}(t_1)$. According to the Lemma 2, $\lambda_2(\beta Q(t_0)+2PH)(t_0) \leq \lambda_2(\beta Q(t_1)+2PH)(t_1)$ can be obtained. Applying this result to all $t_k (k \geq 2)$ moments, we get the following description

$$\begin{aligned} \lambda_2(\beta Q + 2PH)(t_k) &\geq \lambda_2(\beta Q + 2PH)(t_{k-1}) \\ &\geq \lambda_2(\beta Q + 2PH)(t_0). \end{aligned} \tag{27}$$

Therefore, the derivative of $H(t)$ in the interval $[t_{k-1}, t_k)$ can be obtained

$$\begin{aligned} \dot{\Psi}(t) &\leq -\left(\lambda_2\left(\beta Q + 2PH\right)(t_{k-1}) - 4mf\right)\|\tilde{v}\|^2 \\ &\leq -\left(\lambda_2\left(\beta Q + 2PH\right)(t_0) - 4mf\right)\|\tilde{v}\|^2 \\ &\leq 0, \forall t \in [t_{k-1}, t_k). \end{aligned} \tag{28}$$

Hence, there exists $\Psi(t_k) \leq \Psi(t_{k-1}) \leq \Psi_{max}), \forall t \in [t_{k-1}, t_k)$. This result also indicates that existing topology connections in the system will not be disconnected in the interval $[t_{k-1}, t_k)$, but a limited number (N_k) of new communication connections will be added at time t_k. The newly established communication connection will satisfy the following equation:

$$\begin{aligned} N_k &\leq \frac{2mN - m^2 + m}{2} - N \\ N_0 + \cdots + N_k &\leq \frac{2mN - m^2 + m}{2} \end{aligned} \tag{29}$$

Obviously, $\Psi(t_k) \leq \Psi(t_0) + (N_1 + N_2 + \cdots + N_k) V_{max} \leq \Psi_{max}$ can be guaranteed. For a limited number of vehicles in a platoon, the number of topology connection is limited. Therefore, the number of topology switches is also limited. Assume that the vehicle platoon system establishes a stable connection topology at time t_k. Then the string stability of vehicle platoon will be analyzed over interval $[t_k, \infty)$. Based on the above analysis, we know that the length of the communication connection satisfies the following constraints

$$\begin{cases} \tilde{x}_{ij} \geq \min\left\{\tilde{V}_{ij}^{-1}(\Psi_{max})\right\} \\ \tilde{x}_{ij} \leq \max\left\{\tilde{V}_{ij}^{-1}(\Psi_{max})\right\}. \end{cases} \tag{30}$$

Define a following set:

$$\mathrm{S} = \left\{\tilde{x} \in D_1, \tilde{v} \in \mathbb{R}^{N\times N} | \Psi(\tilde{x}, \tilde{v}) \leq \Psi_{max} \quad \right\} \tag{31}$$

where $D_1 = \left\{ \tilde{x} = \mathbb{R}^{N\times N} | \tilde{x}_{ij} \in \begin{bmatrix} \min\left\{\tilde{V}_{ij}^{-1}(\Psi_{max})\right\} \\ \max\left\{\tilde{V}_{ij}^{-1}(\Psi_{max})\right\} \end{bmatrix} \right\}$.
$\forall (i,j) \in \mathcal{G}(t_n)$

According to LaSalle's invariance principle, state trajectory of this vehicle platoon system will converge to the following set:

$$\mathrm{S}_{\mathrm{end}} = \left\{\tilde{x} \in D_1, \tilde{v} \in \mathbb{R}^{N\times N} | \dot{\Psi}(\tilde{x}, \tilde{v}) = 0 \quad \right\}. \tag{32}$$

Substituting $\dot{\Psi}(\tilde{x}, \tilde{v}) = 0$ to (28) , $\tilde{v} = 0$ is obtained, i.e.,

$$v_1 = \cdots = v_N = v_0. \tag{33}$$

Hence, $\frac{\mathrm{d}\|x_{ij}\|_2^2}{\mathrm{d}t} = 2x_{ij}^{\mathrm{T}}(v_i - v_j) = 0$, which means the distance between vehicle i and vehicle j will achieve asymptotically stable.

According to the initial condition, v_0 is constant speed, and combined with (33), we have

$$a = -\begin{bmatrix} \sum_{j\in\mathcal{N}_l\cup\{l\}} \nabla_{\tilde{x}_1}\tilde{V}_{1j} \\ \vdots \\ \sum_{j\in\mathcal{N}_l\cup\{l\}} \nabla_{\tilde{x}_N}\tilde{V}_{Nj} \end{bmatrix} = 0. \tag{34}$$

(34) shows that the vehicle platoon converges gradually to the geometric configuration corresponding to the extreme point of the global field function. However, only the equilibrium points corresponding to the local minimum points are stable equilibrium points, so the final geometry of the vehicle platoon minimizes the global potential function corresponding to each vehicle. Because the potential field function is non-negative over the interval (l_j, ρ), according to the (34), $\tilde{V}_{ij} = 0$ is obtained, which means $\tilde{x}_{ij} = \hat{S}_{ij}$, and $e_i = 0$. Hence, (26) is satisfied, which means the platoon system is ATSS and the distance between vehicle i and vehicle j will converge to the desired value. ■

Algorithm 1 enables the implementation of the distributed control protocol proposed in this section. For each follower vehicle in the vehicle platoon system, this algorithm will be used to achieve cooperative platooning.

Algorithm 1 Distributed controller of each vehicle i

Input: Position and velocity of neighboring vehicles, x_j, and v_j

Output: Control input u_i for vehicle i.

1: Initial Ψ_{max} according to (12).
2: Receive the x_j, v_j, x_0, and v_0 within the communication range of vehicle i.
3: **for** each vehicle j within the communication range.
4: Calculate $\hat{S}_{ij}$ according to (2).
5: Calculate the gradient $\nabla x_i V_{ij}$ of (11).
6: **End for**
7: Calculate the control input u_i according to (10)
8: **Return** Control input u_i

Remark 1: Some methods based on spring-mass-damper have been applied to connected vehicle platoon control. For example, [46] uses a novel control scheme including the inter-distance reference model. It transforms the longitudinal control problem to a tracking problem of the inter-distance reference signal. But this method does not consider the degradation problem of CACC. In the traditional spring-mass-damper methods, the controller parameters are designed from a mechanical perspective. Stabilization and platooning of the vehicle platoon system can be achieved by setting the appropriate spring constant and the damping coefficient. However, due to the linear superposition characteristics of the spring-mass-damping, these controllers may cause very large control inputs to the vehicle, which should be avoided in real-world

applications. In addition, these approaches cannot ensure the preservation of topology connectivity in the vehicle platoon system. On the contrary, our proposed spring damping energy model considers the car row system from the perspective of energy and dissipative system. We design a nonlinear bounded interaction function to ensure the boundedness of the vehicle control input. Besides, it is demonstrated that the topological connectivity of the vehicle platoon system is maintained and enhanced under our control algorithm.

C. Robustness to V2V Communication Loss

Under the framework of the traditional CACC algorithm, the stability of the platoon highly relies on V2V communication. Once V2V communication is lost due to hardware faults, CACC will degenerate into ACC, thus increasing the risk of vehicle collision [38]. As we know, when vehicle i in CACC status degenerates into ACC status, the vehicle i lacks the state information of vehicle $i-2$ out of radar field of view. Once vehicle $i-2$ has a rapid and unexpected deceleration, vehicle $i-1$ may have enough time to respond to braking or deceleration. However, vehicle i may not be able to complete braking or deceleration in a short time because it cannot recognize the unexpected behavior until the completion of vehicle $i-1$ response. However, V2V communication loss is widespread in practical applications. The causing reasons could be hacking, malfunctioning communications equipment, or jammers [21]. This section will analyze how the distributed control algorithm based on the spring damping energy model can resist V2V communication loss.

Suppose that the V2V communication connection between vehicle i and vehicle $i+2$ is lost, which means that spring $K_{i,i+2}$ and the damping element $c_{i,i+2}$ breaks off in the corresponding spring damping energy model (shown in Fig. 3). When $K_{i,i+2}$ breaks, the energy stored in $K_{i,i+2}$ disappears, which means that the total current energy of the system decreases. Since the total system energy is decreasing, the energy stored in the other springs can never exceed the upper limit of the spring's energy storage. This proves that the distance between the two agents is still no less than the compression limit of the spring and no more than the tensile limit. Therefore, for the platoon system, when the communication between vehicle $i+2$ and vehicle i is lost, vehicle $i+2$ can still maintain the topological connection with vehicle $i+1$ through the front radar, and at the same time ensure that the vehicle will not collide with vehicle i, which is not achieved by the existing CACC algorithm.

We reiterate two of critical preconditions of Theorem 1 and Theorem 2. The initial connection topology of the vehicle platoon $\mathcal{G}(t_0)$ is connected and the initial system energy $\Psi(t_0)$ is bounded. Assume that V2V communication is lost in some vehicles of the vehicle platoon system. Then the CACC state will degrade to the ACC state. The vehicle can only obtain the status information of the vehicle in front through the onboard sensors, thus establishing the simplest directional topology connection. The connection topology still satisfies the precondition that the initial topology is connected. When CACC degrades, the number of topology connections of the platoon system will decrease. According to the definition of (12), the total energy of the system will decrease when the topological connections are reduced. Hence, the total energy of the platoon system still satisfies the condition that the energy is bounded. Therefore, Theorem 1 and Theorem 1 and Theorem 2 still hold despite the loss of communication, which means that the stability of the vehicle platoon, the connectivity between vehicles, and collision avoidance can always be guaranteed under the proposed protocol (10).

IV. Experimental Verification

In this section, we focus on verifying the effectiveness of the proposed theoretical results through simulation experiments. We use MATLAB and Unreal Engine for the simulation experiments. In Unreal Engine, the evolution of the vehicle platoon system can be observed visually. We consider how the algorithm performs with different communication topologies and how it works in the case of V2V communication loss. The parameters used in the simulation experiments are given as follows:

- The vehicle platoon consists of five followers and one leader. The initial connection topology of vehicles platoon is connected.
- The communication range of a vehicle ρ is 17 m, and a communication link can be established between vehicle once the distance is less than 17 m.
- The desired distance between the front bumper of each vehicle and the back bumper of its adjacent vehicle ahead is 4 m, and the vehicle body length is 4 m.
- The leader's speed is 6 m/s and the initial speed of each following vehicle is obtained randomly in interval $[2, 6]$ m/s. The maximum velocity of each vehicle v_{max} is 30 m/s.
- The sampling time is 0.025 s, control gain $\beta = 10$, $\xi_1 = \xi_2 = 2$, $c_1 = c_2 = 2$. Furthermore, we determine the $\Psi_{max} = 10$ according to (12).

In addition, in this section, we introduce time-to-collision (TTC) [47] notion to evaluate the safety of the vehicle platoon system. TTC is defined as:

$$TTC_i(t_k)\begin{cases}\frac{x_{i-1}(t_k)-x_i(t_k)-l_{i-1}}{v_i(t_k)-v_{i-1}(t_k)} & \text{if } v_i(t_k) > v_{i-1}(t_k)\\ \infty & \text{if } v_i(t_k) \le v_{i-1}(t_k)\end{cases}. \tag{35}$$

TTC indicates the time for the collision of two consecutive vehicles in the same lane to occur if they maintain their current velocity when the vehicle $i-1$ in front of them is moving slower than i. A smaller TTC value characterizes a more dangerous traffic condition.

A. Case 1: Dynamic Topology

In this case, the effectiveness of the algorithm under dynamic network topology is verified. All the vehicle will disconnect or establish new communication connections in real-time, depending on the status of the surrounding vehicles. Note that the number of topological connections characterizes the system's stability to a certain extent, so in the case of dynamic topology, the increase of the system communication

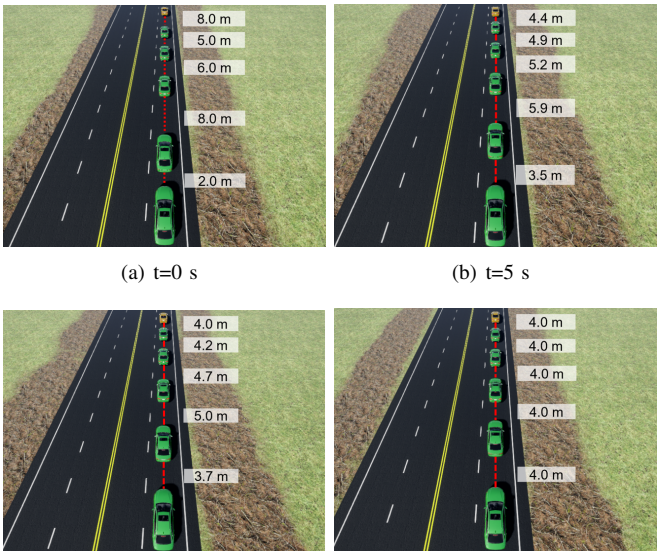

(a) t=0 s (b) t=5 s

(c) t=10 s (d) t=40 s

Fig. 4. Process of the vehicle platooning task under dynamic network topology. The yellow car denotes the leader, and green cars represent the followers.

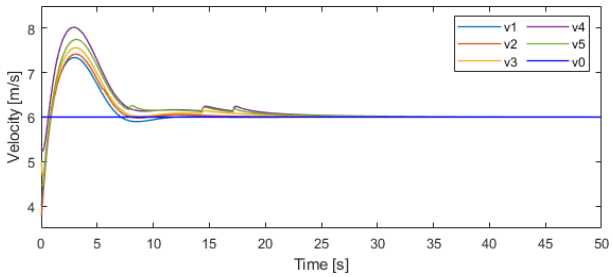

Fig. 5. Time-variation of the velocities of the vehicles, where v_0 represents the velocity of the leader and v_1-v_5 represent the velocities of 5 followers.

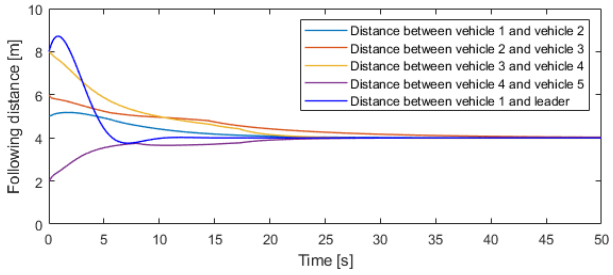

Fig. 6. Time-variation of the vehicle following distances, where the length of the vehicle is defined as 4 m and the desired distance between the vehicle head and the rear of the vehicle in front of it is set as 4 m.

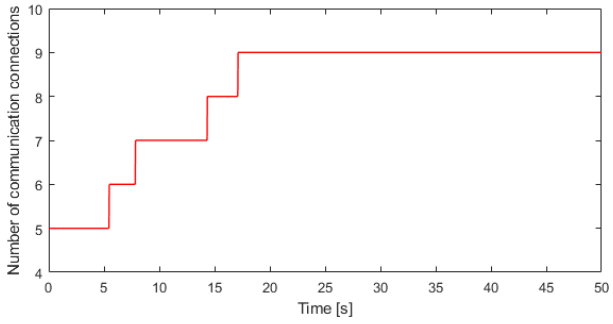

Fig. 7. Time-variation of the number of communication connections.

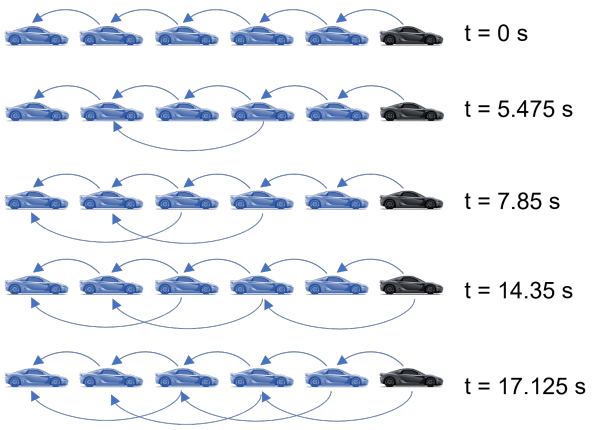

Fig. 8. The dynamic vehicle communication network topology at certain time instant.

connections is beneficial for the stability of the vehicle platoon system.

Fig. 4 depicts the evolution of the entire vehicle platoon system. It is intuitive to see that with the application of the CACC algorithm proposed in this paper, the vehicle successfully forms a stable vehicle platoon system with a safe following distance. Fig. 5 indicates the velocity changes of vehicle platoon for dynamic network topology. The result shows that the velocity of every follower can converge to the velocity of the leader. There is an apparent phenomenon of a sudden change in the speed of the vehicle as it converges. According to our analysis of the experimental results, the abrupt change in speed is mainly caused by the new communication connections. It is clear from the control protocol (10) that when a new communication connection is added at the moment t_k, the vehicle's control input at the moment t_k will suddenly increase or decrease. From Fig. 6, the following distance will also converge to the desired value which is defined as 4 m. Meanwhile, we can note that the following distance is always greater than 2 m, which means the vehicle will never be in a collision with its neighbors. In addition, the communication connection topology of the vehicle platoon changes dynamically as the following distance changes. As can be seen in Fig. 7, the initial number of connections in the platoon is 5, and after t = 17.15 s, the number of connections in the platoon rises to 9 connections. This also means that the convergence speed and stability of the whole platoon system are improved. We can also observe the process of generating new connections for the vehicle platoon in Fig. 8. From all these figures, it is now concluded that the desired vehicle platooning is achieved under the influence of the dynamic network topology.

B. Case 2: Fixed Topology with V2V Communication Loss

In this subsection, we verify the effectiveness of the algorithm for fixed network topology. Here, a worst-case

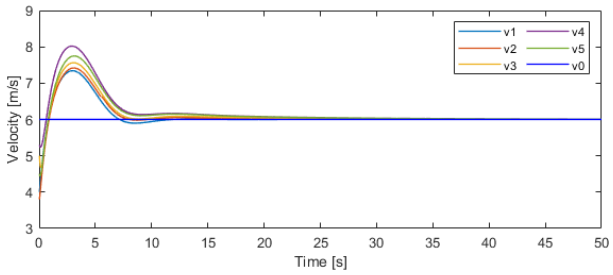

Fig. 9. Time-variation of the velocities of the vehicle platoon without V2V communication.

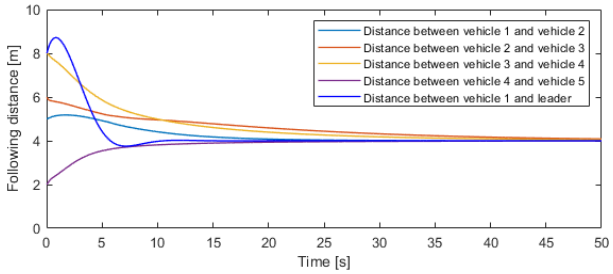

Fig. 10. Time-variation of the vehicle following distances without V2V communication.

fixed topology is considered, e.g., V2V communication is completely disabled, and the topological connection between vehicles is only achieved by the onboard radar, i.e. the vehicle can only acquire the position and speed information of the closest vehicle ahead. The connection topology is as shown in Fig. 8 at moment $\mathrm{t} = 0$ s. With this fixed communication topology, the results in Fig. 9 and Fig. 10 show that the speed and following distance of the vehicle platoon still converge to the desired values although the CACC completely degrades to an ACC. Unlike dynamic topologies, the fixed topology does not experience sudden speed changes under this control protocol (10). This scenario is of great practical importance. When the vehicle platoon is subject to network attacks or communication blocking, the energy model and distributed control protocol proposed can ensure that the vehicle platoon continues to converge safely to a steady state. However, the negative impact of communication loss is also obvious, i.e., it reduces the system convergence speed. A careful comparison of Fig. 6 and Fig. 10 shows that the following distance of the vehicle platoon system converges to the desired value more quickly in the CACC state.

C. Case 3: Vehicle Platoon Merging

Vehicle merging is a common driving scenario. The merging of two different vehicle platoon systems can cause a shock to the original system. Therefore, the CACC algorithm must ensure that multiple vehicle platoon systems are safe and reliable during the merging process. As shown in Fig. 11, for this scenario, we selected two initial vehicle platoon systems that did not enter the steady state. Both platoon systems have their leaders, and when the left platoon system merges into the right platoon, the leader of the left platoon system automatically becomes the follower of the new platoon system.

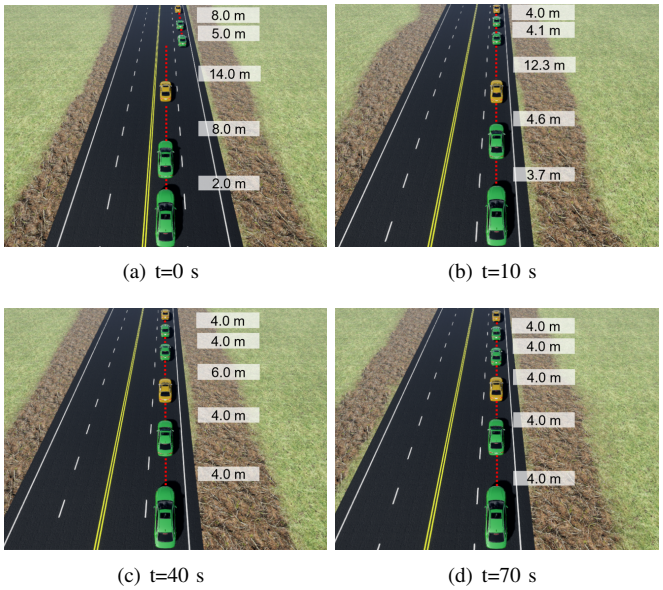

(a) t=0 s (b) t=10 s

(c) t=40 s (d) t=70 s

Fig. 11. Two vehicle platoons merge and form a new platoon system. The yellow car denotes the leaders of two initial vehicle platoons, and green cars represent the followers.

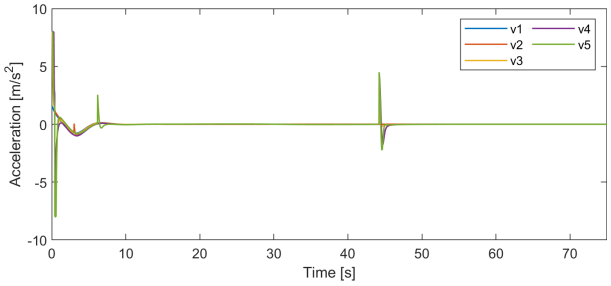

Fig. 12. Time-variation of acceleration of the two vehicle platoons merging process.

The new platoon system gradually converges to the same velocity as the leader and maintains the desired following distance. Figures 12, 13, 14, and 15 show the process of changing vehicle acceleration, velocity, following distance and communication topology connections, respectively. The experimental results fully demonstrate that the CACC algorithm we introduced can achieve a safe and effective merging of two vehicle platoon systems. Note that high peaks can be found in Fig. 13, which are mainly caused by switching communication topology. As can be seen in Fig. 15, two topological connections are established at about t = 45 s, which causes a sudden change in the velocity of the vehicle. At that moment, the acceleration of v4 and v5 is approximately 4.5 $\mathrm{m/s^2}$. The lower and upper bounds of acceleration are -8 $\mathrm{m/s^2}$ and 8 $\mathrm{m/s^2}$, respectively.

D. Case 4: Vehicle Platoon Separating

Another common scenario exists during vehicle platooning, where a vehicle in a CACC state disengages from the current vehicle platoon system. A vehicle platoon system in steady state is bound to leave the original steady state after losing some of its communication nodes. The CACC algorithm must

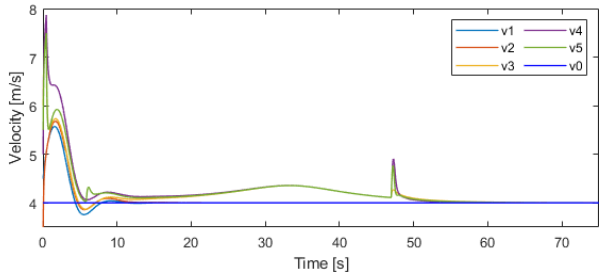

Fig. 13. Time-variation of the velocities of the two vehicle platoons merging process.

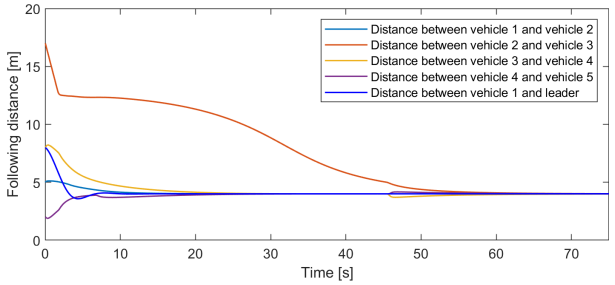

Fig. 14. Time-variation of the following distance of the two vehicle platoons merging process.

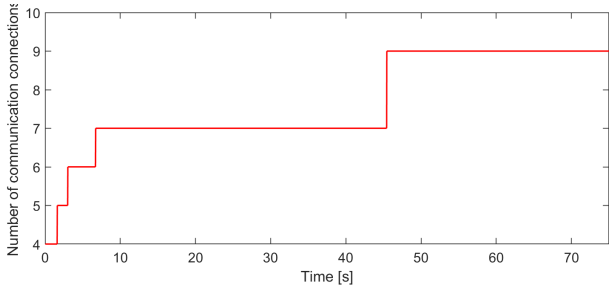

Fig. 15. Time-variation of number of communication connections of the two vehicle platoons merging process.

ensure that the platoon system can form a new steady state in a limited time. As shown in Fig. 16, we consider a scenario where there are two follower vehicles in a steady-state platoon system ready to leave the original platoon, move into the adjacent lane and form a new platoon system. Fig. 16 illustrates the separation of the entire platoon system into two platoon systems and the formation of a new steady state. Fig. 17 and Fig. 18 also show that after the separation of the platoon system, the two newly formed platoon systems also converge to the desired velocity and following distance in a finite time.

E. Case 5: Sudden Velocity Change of the Leader

In this subsection, we explore how the steady-state platoon system responds to the leader's temporary unpredicted acceleration or deceleration. The impact of sudden changes in the leader's speed on the entire platoon system is obvious, which places a high requirement on the string stability of the platoon system. In [48], a distributed predictive control approach was used to implement the string stability of the vehicle platoon.

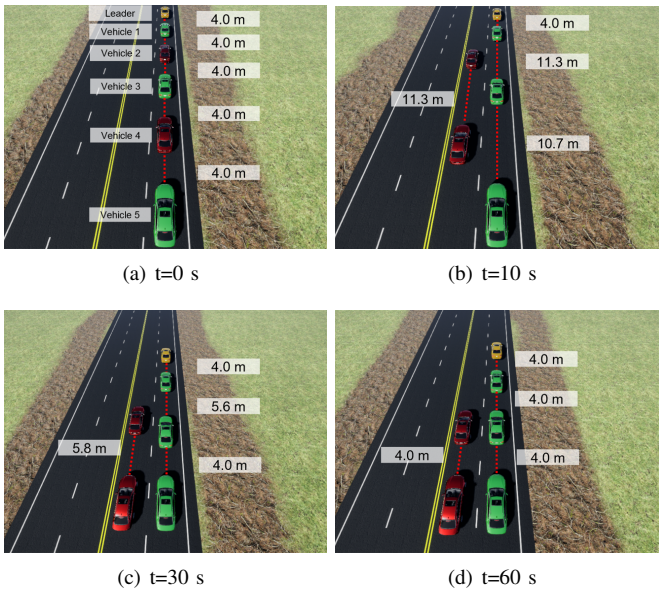

(a) t=0 s (b) t=10 s

(c) t=30 s (d) t=60 s

Fig. 16. Some of the followers break away from the platoon system and form a new platoon. The red cars represent the followers which are out of the platoon.

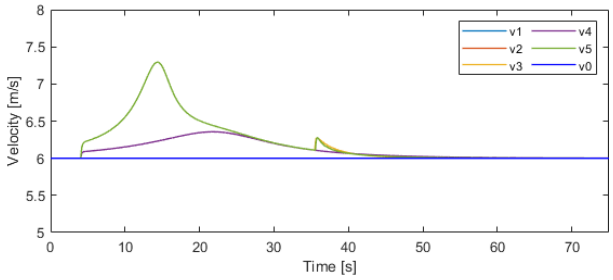

Fig. 17. Time-variation of the velocities of vehicle platoons separating process.

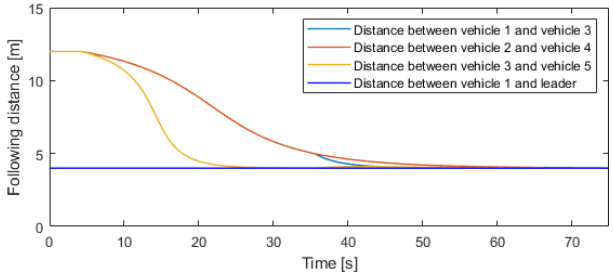

Fig. 18. Time-variation of the following distance of vehicle platoons separating process.

The results demonstrate the effectiveness of the distributed predictive control approach for speed convergence, with the fleet speed responding quickly to changes in reference vehicle speed and converging back to steady state. However, one obvious drawback is that the vehicles travel a different distance when they converge to a new steady state, which means that the vehicle spacing in the platoon does not recover to the desired steady state value. It can be further observed that the spacing between vehicles is increased. The increased following distance of the same platoon of vehicles in two different steady states means that the capacity of the road decreases.

However, such drawback can be overcome by the method proposed in this paper. Fig. 19 (a) and (b) depict the string stability performance of the vehicle platoon under the control protocol proposed in this paper. After a sudden acceleration or deceleration of the leader, the vehicle platoon system is able to converge back to a steady state in a limited time. In addition, the velocity variation shows that the speed of the follower vehicle remains almost synchronized throughout the variation.

F. Comparisons and Discussions

We compare the performance of the proposed method in this paper with the traditional CACC algorithm [49] in scenarios where the leader experienced unintended acceleration or deceleration. The results in Fig. 19 (a) and (c) show that the algorithm proposed in this paper has a faster convergence rate and also a better consistency in the velocity of the followers in the vehicle platoon system. Additionally, Fig. 19 (b) and (d) also indicate that the vehicle platoon system with our algorithm has more stable following distances when the leader experiencing unintended acceleration or deceleration. More importantly, according to the (35), the minimum value of TCC is calculated and shown in Fig. 19 (a) and (c). The results show that our algorithm has a higher TCC value than the traditional CACC algorithm, which means our algorithm is safer.

There are existing control methods that switch between ACC and CACC to address topology changes while still maintaining stability. [50] uses state estimation to deal with the degradation of CACC. This method uses a discrete-time Kalman filter to estimate the object vehicle acceleration and replaces the desired acceleration with the estimated value. Moreover, [51] addresses the degradation of CACC from a communication perspective. This approach requires an extra message-sending function for the vehicle to optimize the information flow topology, thus ensuring fleet stability when CACC degrades. In our paper, we tackle the degradation problem of CACC from the control perspective and propose a control algorithm that can be applied to both CACC and ACC, thus reduce the development cost of the vehicle.

V. Conclusion

In this paper, we proposed a distributed CACC control protocol based on SDEM. Under this control protocol, the vehicle-to-vehicle relationship is defined by a special nonlinear spring and linear damping. Through rigorous mathematical proofs, the stability of the connected vehicle platoon is guaranteed, and vehicle platoon connectivity can be maintained and enhanced during the evolution of the vehicle platoon system. This control protocol enables distance, and speed stabilization of the connected platoon, i.e. the whole platoon will converge to the leader's speed and maintain the desired following distance. The control protocol also enables stable control and maintains the stability of the platoon system in the event of loss of platoon communication. In addition, we simulated a large number of usage scenarios using numerical simulations. The results show that the SDEM and control protocol are suitable for vehicles in the CACC state and also work well for vehicles in the ACC state. Meanwhile, the proposed algorithm ensures the safety and stability of the platoon system for both platoon merging and separation scenarios. For sudden speed shifting of the leader, the vehicle platoon has good string stability. One limitation of this work is that vehicle platoon with time-varying topology may experience abrupt changes in control inputs, which may reduce the comfort of the vehicle. However, we will address and optimize this limitation in our future work.

References

[1] Y. Zhang, Y. Bai, M. Wang, and J. Hu, "Cooperative adaptive cruise control with robustness against communication delay: An approach in the space domain," *IEEE Transactions on Intelligent Transportation Systems*, 2020.

[2] K. C. Dey, L. Yan, X. Wang, Y. Wang, H. Shen, M. Chowdhury, L. Yu, C. Qiu, and V. Soundararaj, "A review of communication, driver characteristics, and controls aspects of cooperative adaptive cruise control (CACC)," *IEEE Transactions on Intelligent Transportation Systems*, vol. 17, no. 2, pp. 491–509, 2015.

[3] A. Alipour-Fanid, M. Dabaghchian, and K. Zeng, "Impact of jamming attacks on vehicular cooperative adaptive cruise control systems," *IEEE Transactions on Vehicular Technology*, vol. 69, no. 11, pp. 12 679–12 693, 2020.

[4] S. Xie, J. Hu, P. Bhowmick, Z. Ding, and F. Arvin, "Distributed motion planning for safe autonomous vehicle overtaking via artificial potential field," *IEEE Transactions on Intelligent Transportation Systems*, 2022.

[5] Y. Kim, J. Guanetti, and F. Borrelli, "Compact cooperative adaptive cruise control for energy saving: Air drag modelling and simulation," *IEEE Transactions on Vehicular Technology*, vol. 70, no. 10, pp. 9838–9848, 2021.

[6] Y. Qin, H. Wang, and B. Ran, "Impacts of cooperative adaptive cruise control platoons on emissions under traffic oscillation," *Journal of Intelligent Transportation Systems*, pp. 1–8, 2019.

[7] S. Knorn, A. Donaire, J. C. Agüero, and R. H. Middleton, "Passivity-based control for multi-vehicle systems subject to string constraints," *Automatica*, vol. 50, no. 12, pp. 3224–3230, 2014.

[8] Y. Wei, C. Avcı, J. Liu, B. Belezamo, N. Aydın, P. T. Li, and X. Zhou, "Dynamic programming-based multi-vehicle longitudinal trajectory optimization with simplified car following models," *Transportation research part B: methodological*, vol. 106, pp. 102–129, 2017.

[9] T. Stanger and L. del Re, "A model predictive cooperative adaptive cruise control approach," in *2013 American Control Conference*. IEEE, 2013, pp. 1374–1379.

[10] R. Schmied, H. Waschl, R. Quirynen, M. Diehl, and L. del Re, "Nonlinear mpc for emission efficient cooperative adaptive cruise control," *IFAC-papersonline*, vol. 48, no. 23, pp. 160–165, 2015.

[11] H. Kazemi, H. N. Mahjoub, A. Tahmasbi-Sarvestani, and Y. P. Fallah, "A learning-based stochastic mpc design for cooperative adaptive cruise control to handle interfering vehicles," *IEEE Transactions on Intelligent Vehicles*, vol. 3, no. 3, pp. 266–275, 2018.

[12] S. Gong and L. Du, "Cooperative platoon control for a mixed traffic flow including human drive vehicles and connected and autonomous vehicles," *Transportation research part B: methodological*, vol. 116, pp. 25–61, 2018.

[13] Y. Zheng, S. E. Li, K. Li, F. Borrelli, and J. K. Hedrick, "Distributed model predictive control for heterogeneous vehicle platoons under unidirectional topologies," *IEEE Transactions on Control Systems Technology*, vol. 25, no. 3, pp. 899–910, 2016.

[14] S. E. Li, Y. Zheng, K. Li, Y. Wu, J. K. Hedrick, F. Gao, and H. Zhang, "Dynamical modeling and distributed control of connected and automated vehicles: Challenges and opportunities," *IEEE Intelligent Transportation Systems Magazine*, vol. 9, no. 3, pp. 46–58, 2017.

[15] Ş. Sabău, C. Oară, S. Warnick, and A. Jadbabaie, "Optimal distributed control for platooning via sparse coprime factorizations," *IEEE Transactions on Automatic Control*, vol. 62, no. 1, pp. 305–320, 2016.

[16] Y. Zhou, S. Ahn, M. Chitturi, and D. A. Noyce, "Rolling horizon stochastic optimal control strategy for acc and cacc under uncertainty," *Transportation Research Part C: Emerging Technologies*, vol. 83, pp. 61–76, 2017.

[17] Y. Zhu, D. Zhao, and Z. Zhong, "Adaptive optimal control of heterogeneous cacc system with uncertain dynamics," *IEEE Transactions on Control Systems Technology*, vol. 27, no. 4, pp. 1772–1779, 2018.

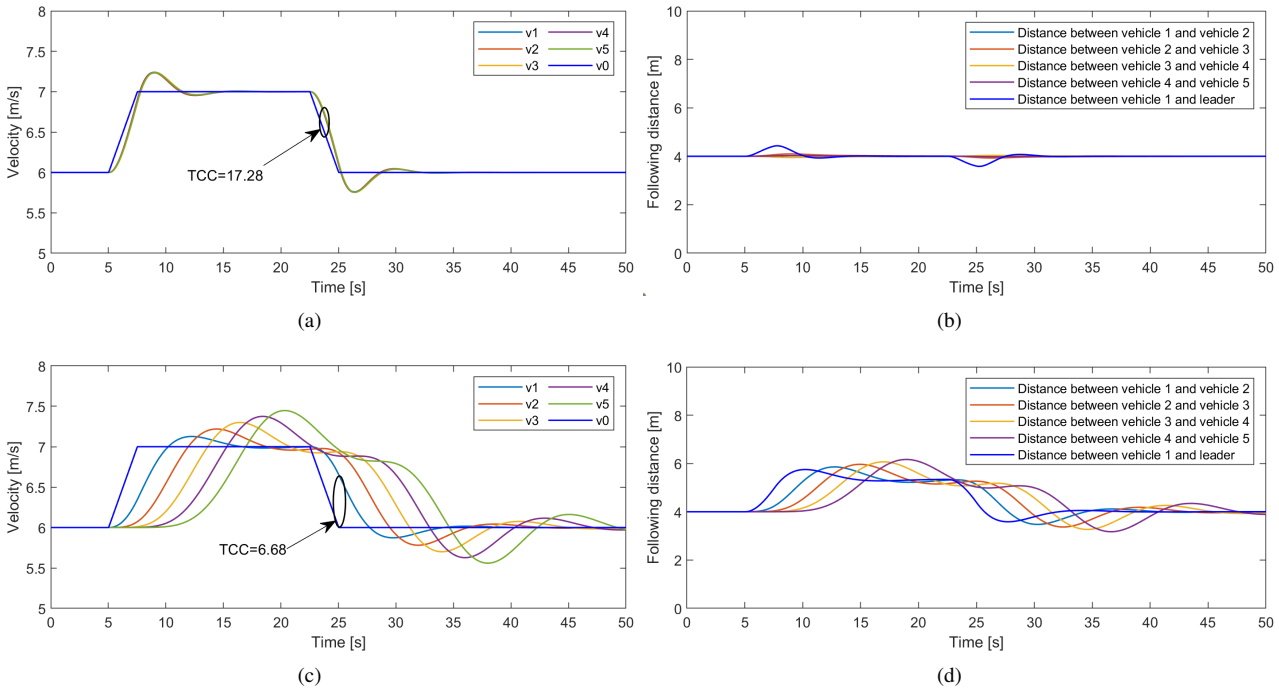

Fig. 19. Simulation results show the performance achieved by the proposed distributed CACC algorithm based SEDM and the traditional CACC algorithm [49] to a platoon of six vehicles of which one acts as the leader while the rest five are followers. (a) Time-variation of the velocities with proposed distributed CACC algorithm based SEDM, (b) Time-variation of the following distance with proposed distributed CACC algorithm based SEDM, (c) Time-variation of the velocities with traditional CACC algorithm, and (d) Time-variation of the following distance with traditional CACC algorithm. In (a) and (c), the minimum value of TCC is calculated and shown.

[18] T. Chu and U. Kalabić, "Model-based deep reinforcement learning for cacc in mixed-autonomy vehicle platoon," in *2019 IEEE 58th Conference on Decision and Control (CDC)*. IEEE, 2019, pp. 4079–4084.

[19] S. Na, H. Niu, B. Lennox, and F. Arvin, "Bio-inspired collision avoidance in swarm systems via deep reinforcement learning," *IEEE Transactions on Vehicular Technology*, 2022.

[20] W. Gao, J. Gao, K. Ozbay, and Z.-P. Jiang, "Reinforcement-learning-based cooperative adaptive cruise control of buses in the lincoln tunnel corridor with time-varying topology," *IEEE Transactions on Intelligent Transportation Systems*, vol. 20, no. 10, pp. 3796–3805, 2019.

[21] Y. G. Dantas, V. Nigam, and C. Talcott, "A formal security assessment framework for cooperative adaptive cruise control," in *2020 IEEE Vehicular Networking Conference (VNC)*. IEEE, 2020, pp. 1–8.

[22] S. Xie, J. Hu, Z. Ding, and F. Arvin, "Collaborative overtaking of multi-vehicle systems in dynamic environments: A distributed artificial potential field approach," in *International Conference on Advanced Robotics (ICAR)*. IEEE, 2021, pp. 873–878.

[23] R. van der Heijden, T. Lukaseder, and F. Kargl, "Analyzing attacks on cooperative adaptive cruise control (cacc)," in *2017 IEEE Vehicular Networking Conference (VNC)*. IEEE, 2017, pp. 45–52.

[24] K. Wu, J. Hu, B. Lennox, and F. Arvin, "Mixed controller design for multi-vehicle formation based on edge and bearing measurements," in *2022 European Control Conference (ECC)*. IEEE, 2022, pp. 1666–1671.

[25] Y. He, M. Makridis, G. Fontaras, K. Mattas, H. Xu, and B. Ciuffo, "The energy impact of adaptive cruise control in real-world highway multiple-car-following scenarios," *European Transport Research Review*, vol. 12, no. 1, pp. 1–11, 2020.

[26] B. Ciuffo, K. Mattas, M. Makridis, G. Albano, A. Anesiadou, Y. He, S. Josvai, D. Komnos, M. Pataki, S. Vass *et al.*, "Requiem on the positive effects of commercial adaptive cruise control on motorway traffic and recommendations for future automated driving systems," *Transportation research part C: emerging technologies*, vol. 130, p. 103305, 2021.

[27] Y. He, K. Mattas, R. Dona, G. Albano, and B. Ciuffo, "Introducing the effects of road geometry into microscopic traffic models for automated vehicles," *IEEE Transactions on Intelligent Transportation Systems*, 2021.

[28] F. Alotibi and M. Abdelhakim, "Anomaly detection for cooperative adaptive cruise control in autonomous vehicles using statistical learning and kinematic model," *IEEE Transactions on Intelligent Transportation Systems*, vol. 22, no. 6, pp. 3468–3478, 2020.

[29] M. Iorio, F. Risso, R. Sisto, A. Buttiglieri, and M. Reineri, "Detecting injection attacks on cooperative adaptive cruise control," in *2019 IEEE Vehicular Networking Conference (VNC)*. IEEE, 2019, pp. 1–8.

[30] V.-L. Nguyen, P.-C. Lin, and R.-H. Hwang, "Enhancing misbehavior detection in 5g vehicle-to-vehicle communications," *IEEE Transactions on Vehicular Technology*, vol. 69, no. 9, pp. 9417–9430, 2020.

[31] G. Bella, P. Biondi, G. Costantino, and I. Matteucci, "Cinnamon: A module for autosar secure onboard communication," in *2020 16th European Dependable Computing Conference (EDCC)*. IEEE, 2020, pp. 103–110.

[32] J. Hu, H. Niu, J. Carrasco, B. Lennox, and F. Arvin, "Fault-tolerant cooperative navigation of networked uav swarms for forest fire monitoring," *Aerospace Science and Technology*, p. 107494, 2022.

[33] Y. Tu, W. Wang, Y. Li, C. Xu, T. Xu, and X. Li, "Longitudinal safety impacts of cooperative adaptive cruise control vehicle's degradation," *Journal of safety research*, vol. 69, pp. 177–192, 2019.

[34] J. Hu, B. Lennox, and F. Arvin, "Robust formation control for networked robotic systems using negative imaginary dynamics," *Automatica*, vol. 140, p. 110235, 2022.

[35] F. Acciani, P. Frasca, G. Heijenk, and A. A. Stoorvogel, "Stochastic string stability of vehicle platoons via cooperative adaptive cruise control with lossy communication," *IEEE Transactions on Intelligent Transportation Systems*, 2021.

[36] J. Sawant, U. Chaskar, and D. Ginoya, "Robust control of cooperative adaptive cruise control in the absence of information about preceding vehicle acceleration," *IEEE Transactions on Intelligent Transportation Systems*, 2020.

[37] P. E. Paré, E. Hashemi, R. Stern, H. Sandberg, and K. H. Johansson, "Networked model for cooperative adaptive cruise control," *IFAC-PapersOnLine*, vol. 52, no. 20, pp. 151–156, 2019.

[38] C. Wu, Y. Lin, and A. Eskandarian, "Cooperative adaptive cruise control with adaptive kalman filter subject to temporary communication loss," *IEEE Access*, vol. 7, pp. 93 558–93 568, 2019.

[39] S. Wei, Y. Zou, X. Zhang, T. Zhang, and X. Li, "An integrated longitudinal and lateral vehicle following control system with radar and vehicle-to-vehicle communication," *IEEE Transactions on Vehicular Technology*, vol. 68, no. 2, pp. 1116–1127, 2019.

[40] C. Zhai, F. Luo, Y. Liu, and Z. Chen, "Ecological cooperative look-ahead control for automated vehicles travelling on freeways with varying slopes," *IEEE Transactions on Vehicular Technology*, vol. 68, no. 2, pp. 1208–1221, 2019.
[41] H. Chehardoli, "Robust optimal control and identification of adaptive cruise control systems in the presence of time delay and parameter uncertainties," *Journal of Vibration and Control*, vol. 26, no. 17-18, pp. 1590–1601, 2020.
[42] S. Gong, A. Zhou, and S. Peeta, "Cooperative adaptive cruise control for a platoon of connected and autonomous vehicles considering dynamic information flow topology," *Transportation Research Record*, vol. 2673, no. 10, pp. 185–198, 2019.
[43] F. L. Lewis, H. Zhang, K. Hengster-Movric, and A. Das, *Cooperative control of multi-agent systems: optimal and adaptive design approaches*. Springer Science & Business Media, 2013.
[44] Z. Qu, *Cooperative Control of Dynamical Systems: Applications to Autonomous Vehicles*. U.K., London: Springer, 2009.
[45] S. Feng, Y. Zhang, S. E. Li, Z. Cao, H. X. Liu, and L. Li, "String stability for vehicular platoon control: Definitions and analysis methods," *Annual Reviews in Control*, vol. 47, pp. 81–97, 2019.
[46] J.-J. Martinez and C. Canudas-de Wit, "A safe longitudinal control for adaptive cruise control and stop-and-go scenarios," *IEEE Transactions on control systems technology*, vol. 15, no. 2, pp. 246–258, 2007.
[47] Y. Li, Z. Li, H. Wang, W. Wang, and L. Xing, "Evaluating the safety impact of adaptive cruise control in traffic oscillations on freeways," *Accident Analysis & Prevention*, vol. 104, pp. 137–145, 2017.
[48] E. van Nunen, J. Reinders, E. Semsar-Kazerooni, and N. Van De Wouw, "String stable model predictive cooperative adaptive cruise control for heterogeneous platoons," *IEEE Transactions on Intelligent Vehicles*, vol. 4, no. 2, pp. 186–196, 2019.
[49] V. Milanés and S. E. Shladover, "Modeling cooperative and autonomous adaptive cruise control dynamic responses using experimental data," *Transportation Research Part C: Emerging Technologies*, vol. 48, pp. 285–300, 2014.
[50] J. Ploeg, E. Semsar-Kazerooni, G. Lijster, N. van de Wouw, and H. Nijmeijer, "Graceful degradation of cacc performance subject to unreliable wireless communication," in *16th International IEEE Conference on Intelligent Transportation Systems (ITSC 2013)*. IEEE, 2013, pp. 1210–1216.
[51] C. Wang, S. Gong, A. Zhou, T. Li, and S. Peeta, "Cooperative adaptive cruise control for connected autonomous vehicles by factoring communication-related constraints," *Transportation Research Part C: Emerging Technologies*, vol. 113, pp. 124–145, 2020.

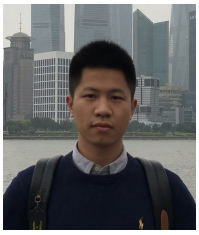

Songtao Xie received the B.Eng. degree in mechanical design as well as manufacturing and its automation from Sichuan University, Chengdu, China, in 2016, and the master's degree in mechanical engineering design from The University of Manchester, U.K., in 2017, where he is currently pursuing the Ph.D. degree. He worked as a Function and System Development Engineer at Geely Automobile Holdings Ltd., from 2017 to 2019. His research interests include multi-vehicle systems, distributed control, and autonomous driving.

Junyan Hu received B.Eng degree in Automation from Hefei University of Technology in 2015 and Ph.D degree in Electrical and Electronic Engineering from the University of Manchester in 2020.

Dr. Hu is currently an Assistant Professor with the Department of Computer Science, University College London (UCL). Prior to joining UCL, he worked as a Research Associate in Robotics at the University of Manchester. His research interests include swarm intelligence, multi-agent systems, cooperative path planning, distributed learning and control, with applications to autonomous driving and robotics. He has been serving as an Associate Editor for IEEE Robotics and Automation Letters and IEEE International Conference on Robotics and Automation. He is a member of IEEE-CSS Technical Committee on Networks and Communication Systems, IEEE-RAS Technical Committee on Multi-Robot Systems, and IFAC Technical Committee on Large Scale Complex Systems.

Zhengtao Ding received the B.Eng. degree from Tsinghua University, Beijing, China, in 1984, and the M.Sc. degree in systems and control, and the Ph.D. degree in control systems from the University of Manchester Institute of Science and Technology, Manchester, U.K. in 1986 and 1989, respectively. After working as a Lecturer with Ngee Ann Polytechnic, Singapore, for ten years, he joined the University of Manchester in 2003, where he is currently Professor of Control Systems with the Dept of Electrical and Electronic Engineering. He is the author of the book: Nonlinear and Adaptive Control Systems (IET, 2013) and has published over 300 research articles. His research interests include nonlinear and adaptive control theory and their applications, more recently network-based control, distributed optimization and distributed machine learning, with applications to power systems and robotics. Prof. Ding has served as an Associate Editor for the IEEE Transactions on Automatic Control, IEEE Control Systems Letters, and several other journals. He is a member of IEEE Technical Committee on Nonlinear Systems and Control, IEEE Technical Committee on Intelligent Control, and IFAC Technical Committee on Adaptive and Learning Systems.

Farshad Arvin received the BSc degree in Computer Engineering, the MSc degree in Computer Systems engineering, and the PhD degree in Computer Science, in 2004, 2010, and 2015, respectively. Farshad is an Associate Professor in Robotics in the Department of Computer Science at Durham University. Prior to that, he was a Senior Lecturer in Robotics at The University of Manchester, UK. He visited several leading institutes including Artificial Life Laboratory with the University of Graz, Institute of Microelectronics, Tsinghua University, Beijing, and Italian Institute of Technology (iit) in Genoa as a Senior Visiting Research Scholar. His research interests include swarm robotics and autonomous multi-agent systems. He is the Founding Director of the Swarm & Computation Intelligence Laboratory (SwaCIL) formed in 2018.